EurJOC
European Journal of Organic Chemistry

A Journal of
ChemPubSoc Europe

Accepted Article

Title: β-Amyrin biosynthesis: Effect of steric bulk at the 6-, 10-, and 15-positions in the 2,3-oxidosqualene backbone on polycyclisation cascades

Authors: Yuri Terasawa; Yusuke Sasaki; Yuki Yamaguchi; Kazunari Takahashi; Tsutomu Hoshino

To be cited as: Eur. J. Org. Chem. 10.1002/ejoc.201601306

Link to VoR: https://doi.org/10.1002/ejoc.201601306

Supported by
ACES Asian Chemical Editorial Society

WILEY-VCH

β-Amyrin biosynthesis: Effect of steric bulk at the 6-, 10-, and 15-positions in the 2,3-oxidosqualene backbone on polycyclisation cascades

Yuri Terasawa, Yusuke Sasaki, Yuki Yamaguchi, Kazunari Takahashi and Tsutomu Hoshino*

Department of Applied Biological Chemistry, Faculty of Agriculture and Graduate School of Science and Technology, Niigata University, Ikarashi 2-8050, Nishi-ku, Niigata, Japan 950-2181

E-mail: hoshitsu@agr.niigata-u.ac.jp

Supporting information for this article is available. on the WWW under …..

Table of Content: Polycyclization cascade

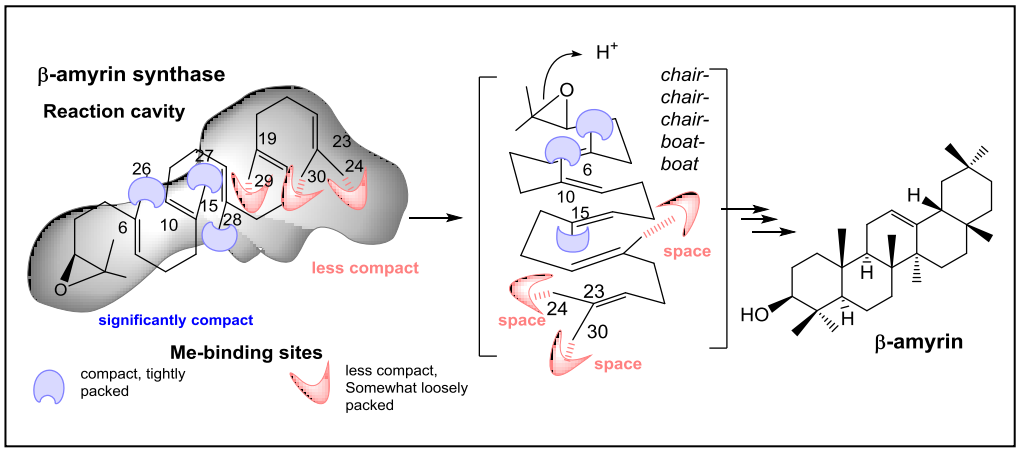

On the methyl binding sites in the reaction cavity of β-amyrin synthase: catalytic domain responsible for the earlier stage of the polycyclization reaction is notably compact, while that for the latter stage is somewhat loosely packed.

Abstract

β-Amyrin synthase incubation experiments were conducted to determine the influence of sterics at the C-6, C-10, and C-15 positions of 2,3-oxidosqualene on the polycyclisation pathway. Nor- and ethyl-substituted oxidosqualene analogues were synthesised. Cyclisation of the ethyl-substituted analogues did not occur, but the nor-analogues underwent a polycyclisation cascade, yielding fully cyclised products with 6/6/6/6/6-fused pentacyclic scaffolds, generated via a final oleanyl cation. Previously, we reported that C-19 and C-23 ethyl-substituted analogues underwent polycyclisation reactions. Therefore, the catalytic site domain involved in earlier cyclisation steps was notably compact. In contrast, the catalytic domain in later cyclisation steps was more loosely packed (less compact) to accommodate the bulky ethyl group. The reaction spaces for recognising branched methyl groups are discussed by comparing β-amyrin synthase with other triterpene cyclases, such as lanosterol and hopene synthases.

Keywords: Alkene; cyclization, enzyme catalysis; polycycle; terpenoids

Introduction

The polycyclisation cascades of squalene and (3*S*)-2,3-oxidosqualene (**1**) have attracted organic chemists and biochemists ever since Ruzicka and coworkers proposed their "biogenetic isoprene rule" more than 70 years ago.[1] The reactions proceed with complete regio- and stereospecificity, yielding sterols and triterpenes with remarkable structural diversity,[2] of which there are more than 100 different carbon frameworks exhibiting important biological activities.[3] β-Amyrin (**2**) is widely found in plants and contains a pentacyclic scaffold with eight chiral centres. Recently, we succeeded in isolating pure β-amyrin synthase from *Euphorbia tirucalli* (EtAS) and characterised its enzymatic properties.[4] β-Amyrin synthase folds oxidosqualene, **1**, into a *chair–chair–chair–boat–boat* conformation (Scheme 1).[1,5] Proton attack at the epoxide ring initiates a polycyclisation reaction, yielding dammarenyl cation **3** containing a 6/6/6/5-fused A/B/C/D-tetracyclic ring system, which then undergoes ring expansion to afford 6/6/6/6-fused tetracyclic baccharenyl cation **4**. Further cyclisation affords 6/6/6/6/5-fused pentacyclic lupanyl cation **5**.

＜Figure 1 & Scheme 1>

A second ring expansion of the five-membered E-ring generates 6/6/6/6/6-fused pentacyclic oleanyl cation **6**. Subsequent 1,2-hydride shifts (H-18α to C-19 cation and H-13β to C-18) and deprotonation of H-12α, introduces a double bond between C-12 and C-13, finally generating the β-amyrin skeleton (Scheme 1). The enzymatic reactions of substrate analogues with β-amyrin synthase have been reported,[6–9] but little is known about the effect of steric bulk at the methyl-group position in **1** on the polycyclisation cascade. We have reported the polycyclisation reactions of substrate analogues **13**–**18** and 24,30-bisnoroxidosqualene using EtAS enzyme.[10–12] The 23*Z*-methyl group is critical for the correct folding of **1** to yield **2**,[11] with large amounts of tetracyclic products formed in its absence, resulting from the polycyclisation cascade terminating at the intermediate stage. In contrast, the absence of the 23*E*-Me group had little influence on the polycyclisation cascade, with the β-amyrin skeleton afforded in approx. 96% yield. We previously proposed that a CH–π interaction operates between 23*Z*-Me and the binding site.[12] A larger ethyl group is also tolerated at the C-23 position, furnishing the β-amyrin skeleton irrespective of whether the *E*- (**15**) or *Z*-substituted (**16**) analogue is used.[12] Ethyl group substitution at the 19-position in **14** is also tolerated, with polycyclisation affording the β-amyrin skeleton and 6/6/6/5-fused tetracyclic skeleton in a 1:3 ratio.[10] Furthermore, 29-noroxidosqualene (**13**) afforded a novel scaffold consisting of a 6/6/6/6-fused tetracycle. However, the effects of changing sterics at the 6-, 10-, and 15-positions of **1** on the polycyclisation have not been reported. Herein, we describe the polycyclisation cascades of **7**–**12**, showing that ethyl-substituted oxidosqualenes **7**–**9** underwent no reaction, while noroxidosqualenes **10**–**12** afforded oleanyl cation-derived products. The reaction spaces for recognising branched methyl groups are discussed by comparing β-amyrin synthase with other triterpene cyclases, such as lanosterol and hopene synthases.

Results

Syntheses of substrate analogues 7–14.

*Synthesis of substrate analogues: Ethyl-substituted oxidosqualenes **8** and **9***

The starting material, C_{17}-aldehyde **19**, was prepared according to our previous report.[13] Squalene was treated with *m*CPBA (*m*-chloroperbenzoic acid) in CH_2Cl_2 to produce an epoxide mixture, which was then treated with H_5IO_6, yielding a mixture of C_{17}-**19**, C_{22}-**20**, and C_{27} aldehydes. Scheme 2A shows the synthetic design of **8** and **9**. Aldehyde **19** was subjected to a Wittig–Horner reaction using triethyl

2-phosphonobutyrate to yield an *E/Z*-mixture of alkenes, which were separated by SiO_2 column chromatography to isolate *E*-isomer **21**. Compound **21** was reduced with DIBAL-H to give alcohol **22**, which was then converted to bromide **23** using PBr_3. Geraniol (**26**) was also transformed into the corresponding bromide using PBr_3, followed by treatment with sodium benzenesulfinate, to afford phenylsulfone derivative **27**. Compound **27** was then converted to a bromohydrin using *N*-bromosuccinimide (NBS), and subsequent epoxide **28** using K_2CO_3. Compounds **23** and **28** were subjected to a coupling reaction using *n*-BuLi, yielding the phenylsulfone derivative of ethyl-substituted analogue **29**. To remove the phenylsulfonyl group, **29** was treated with Super-Hydride reagent, yielding desired compound **8**. Alcohol **22** was also treated with NBS to give bromohydrin **24**, which was then transformed into bromide **25**. The coupling reaction of **25** and **27** gave **30**, which was treated with Super-Hydride reagent to afford desired compound **9**.

<Scheme 2>

*Synthesis of substrate analogues: A mixture of ethyl-derivatives **7** and **14** and that of nor-derivatives **10** and **13**.*

Ethyl- and nor-derivatives were prepared using similar synthetic procedures to those for **8** and **9**, with the synthetic plans shown in Scheme 2B. To prepare ethyl-substituted **7** and **14**, aldehyde **20** was first converted into alkene **31** using triethyl 2-phosphonobutyrate. Next, **31** was reduced to alcohol **33**, which was then treated with PBr_3 to afford bromide **35**. Commercially available 3-methylbut-2-en-1-ol (**37**) was transformed into phenylsulfone **38**, as detailed in our previous report.[13] The coupling reaction of **35** and **38** yielded **39**. Desulfonation was carried out using Super-Hydride reagent to afford **41**. Subsequent reactions of **41** with NBS and K_2CO_3 furnished a mixture of **7** and **14** in an approx. 1:1 ratio (Supporting Information, Figs. S2–S5). To prepare noroxidosqualenes **10** and **13**, triethyl 2-phosphonoacetate was employed in the Wittig–Horner reaction to produce **32**. Subsequent reactions to prepare the mixture of **10** and **13** were the same as those to prepare **7** and **14**. The final ratio of **10** and **13** was also approx. 1:1 (Figs. S6–S8)

Details of the preparation of synthetic intermediates and their characterisation by NMR and MS are given in Supporting Information. In particular, detailed NMR analyses are given for the mixtures of **7** and **14,** and **10** and **13** (Supporting Information, pp. S11–S16).

Enzymatic reaction of 7–14 with β-amyrin synthase

A buffered reaction mixture (2.5 mL, pH 7.4, 100 mM potassium phosphate buffer), consisting of Triton X-100 (0.1%, *w*/*v*), **1** [200 μg, (3*R*/*S*)-racemic mixture], BSA (1 mg/mL), DTT (dithiothreitol, 1 mM), and purified histidine-tagged EtAS (5 μg), was incubated at 30 °C for 9 h.[4,12] Next, 15% KOH/MeOH (7.5 mL) was added, and the resulting mixture was heated to 70–80 °C for 30 min. The lipophilic materials were extracted with hexane, and 20 μg of squalene was added to the hexane extract as the internal standard. Triton X-100 present in the extract was removed by elution through an SiO_2 column (hexane/EtOAc, 100:10), and the eluent was evaporated to dryness. Next, hexane (150 μL) was added to the residue and 1.0 μL of the resultant solution was subjected to GC analysis in order to quantify the lipophilic materials. Several peaks corresponding to oxidosqualene (**1**) and its analogues (**7**–**14**) indicated that these substrates were thermally degraded during GC analyses (see Figs. 2 and S9).

Figure S9 depicts GC analyses obtained from incubation of the ethyl-substituted analogues of **8**, **9**, **14**, and the mixture of **7** and **14**. No conversion of **8** and **9** was observed. In contrast, analogue **14** was transformed into **47** and **48** (1:3 ratio), as we reported previously.[10] Incubation results for a mixture of **7** and **14** indicated that only products **47** and **48** were produced. Furthermore, the product peak areas of only **14** and the mixture of **7** and **14** were indistinguishable in the GC profile. Therefore, substrate **7** underwent no or little transformation.

Figure 2 shows the GC profiles of the hexane extract obtained from incubation experiments of **1**, **11**–**13**, and the mixture of **10** and **13**. Unlike the ethyl-substituted analogues, these nor-analogues underwent enzymatic reactions, forming cyclic products. Figure 3 shows the relative conversion yields of substrate analogues **7**–**14** relative to that of **1**. As these synthesised analogues were (3*R*/*S*)-racemic mixtures, and only the cyclisation reaction of (3*S*)-oxidosqualene proceeds, the conversion yields were calculated as twice the value of the GC peak areas. Compound **11** was converted into **49**–**51** in a substantial yield (34%). Analogue **12** was also transformed into **52**–**54** in a fair yield (22%). However, the reaction yield of **55** from **13** was poor (3.4%), due to the occurrence of time-dependent inhibition of this reaction, as described in our previous report.[10] Incubation of a mixture of **10** and **13** generated **56** in a negligible yield (0.8%), in addition to **55**, suggesting that time-dependent inhibition caused by **10** was stronger than that of **13**.

<Figures 2 & 3>

Product isolation and chemical structure elucidation.

Analogue **11** (50 mg) was incubated with partially purified β-amyrin synthase (30 mg) under optimal conditions. The lipophilic materials, including the enzymatic products and unreacted **8**, were extracted with hexane, and Triton X-100 present in the hexane extract was removed by elution through a short SiO_2 column (hexane/EtOAc, 100:20). In subsequent SiO_2 column chromatography (*n*-hexane/EtOAc, 100:0–100:5), substrate **11** was eluted first, with a yield of 4.0 mg, with a fraction containing a mixture of enzymatic products collected subsequently. The latter fraction (12.6 mg) was converted into acetates with Ac_2O/Py, and subjected to separation by normal phase HPLC (*n*-hexane/THF, 100:2), affording pure **50** (6.5 mg). Separation of the mixed fraction containing **49** and **51** was also successful using HPLC (*n*-hexane/THF, 100:2), giving isolated yields of 0.8 and 0.1 mg for **51** and **49**, respectively. Analogue **12** was also incubated under similar conditions, and acetate products were isolated by normal phase HPLC, affording **53** (2.83 mg), **52** (0.66 mg), and **54** (0.52 mg).

We reported the structures of **47** and **48** previously (Fig. 4).[10] The structures of products **49**–**54** were determined by detailed NMR analyses. The NMR spectra, including ^1H, ^{13}C, ^1H–^1H COSY, HOHAHA, NOESY, HSQC, and HMBC experiments, are included in Figs. S10–S15. DEPT 45, 90, and 135 spectra were also measured to differentiate methyl, methylene, methine, and quaternary carbons. In the ^{13}C NMR spectrum of product **49** acetate (150 MHz, C_6D_6), one double bond was found at δ_C = 137.7 (s) and 131.6 (s), but no olefinic protons were observed in the ^1H NMR spectrum (600 MHz, C_6D_6). Me-26 (δ_H 1.20, 3H, s) and Me-27 (δ_H 1.23, s, 3H) had clear HMBC cross-peaks with δ_C 137.7 (s) and 131.6 (s), respectively, indicating that the double bond was located at C-13/C-18. A clear nuclear Overhauser effect (NOE) was observed between Me-27 and Me-29 (δ_H 1.12, s, 3H), and between Me-26 and H-9 (δ_H 1.06, m, 1H). These findings confirmed the assignments of Me-26, Me-27, and Me-29. Me-27 was β-oriented, because unambiguous NOEs were found for Me-29 and H-19β (1.89, m, 1H), H-19β and Me-27, and H-19β and H-12β (1.83, m, 1H). The presence of a 1,1-dimethylcyclohexane ring (E-ring) was confirmed as follows: Me-28 (δ_H 0.978, s, 3H; δ_C 24.1, q) and Me-29 (δ_C 32.6, q) showed strong NOE and HMBC correlations with each other. Furthermore, both Me-28 and Me-29 had definitive HMBC cross-peaks for C-20 (δ_C 33.4, s), C-19 (δ_C 38.9, t), and C-21 (δ_C 35.8, t). Thus, the polycyclisation reaction proceeded toward the final stage without truncation of the polycyclisation cascade. Me-26 had a strong HMBC correlation with C-8 (δ_C 48.7, d), indicating a hydrogen atom substituent at C-8, which was further supported by the definitive NOE between H-8 (δ_H 1.18, m, 1H) and Me-25 (δ_H 0.810, s, 3H). Detailed NMR analyses of acetate **49** (Fig. S10.9) allowed us to determine **49** to be 26-nor-δ-amyrin, as shown in

Figs. 4 and S10.9.

<Figure 4>

One double bond was also found in the ^{1}H (400 MHz, C_6D_6) and ^{13}C NMR spectra (100 MHz, C_6D_6) of product **50** acetate: δ_H 5.47 (t, J = 3.6 Hz, 1H, H-12); δ_C 123.1 (d, C-12), and δ_C 146.2 (s, C-13). The double-bond position was confirmed by HMBC correlations between Me-26 (δ_H 1.17, s, 3H) and C-13, and H-18 (δ_H 2.23, m, 1H) and C-12/C-13. Strong NOEs were observed for Me-29 (δ_H 1.17, s, 3H) and H-18, and Me-27 (δ_H 1.07, s, 3H) and H-18, supporting the assignment of the β-amyrin skeleton in **50** acetate. However, the C-8 Me group in β-amyrin had been replaced with a hydrogen atom, determined by observation of a strong NOE for Me-25 (δ_H 0.840, s, 3H) and H-8 (δ_H 1.34, m, 1H), and a clear HMBC cross-peak for Me-26 and C-8 (δ_C 44.8, d). All detailed NMR analyses (Fig. S11.9) verified that **50** was 26-nor-β-amyrin, as depicted in Figs. 4 and S11.9.

One double bond was found in the ^{1}H (600 MHz, C_6D_6) and ^{13}C NMR spectra (150 MHz, C_6D_6) of **51** acetate: δ_H 5.19 (s, 1H); δ_C 129.9 (d, C-19), and 142.4 (s, C-18). Definitive HMBC correlations between Me-27 (δ_H 1.23, s, 3H) and C-18, Me-29 (δ_H 1.20, s, 3H) and C-19, and Me-28 (δ_H 1.20, s, 3H) and C-19 demonstrated that the double bond was positioned at C-18/C-19. The following definitive NOEs were observed: Me-27/H-13 (δ_H 1.94, bd, J=11.8 Hz, 1H), H-13/H-8 (δ_H 1.17, m, 1H), H-8/Me-25 (δ_H 0.882, s, 3H), and Me-26 (δ_H 0.817, s, 3H)/H-9 (δ_H 0.92, m, 1H), indicating the structure and stereochemistry shown in Fig. 4, with compound **51** determined to be 26-norgermanicol. Detailed analyses of the NMR data are shown in Fig. S12.9.

^{1}H (600 MHz) and ^{13}C NMR spectra (150 MHz) of **52** acetate were measured in C_6D_6. Acetylated **52** also contained one double bond at δ_C 130.0 (s, C-13) and 135.5 (s, C-14), but no olefinic protons were found. The double-bond position was determined by detailed HMBC analyses, showing that C-14 had definitive cross-peaks with the following protons via 3-bond C-H couplings: H-9 (δ_H 1.03, m, 1H), Me-26 (δ_H 1.10, s, 3H), H-16 (δ_H 1.05, m, 1H; δ_H 2.10, m, 1H). Me-26 was determined to be β-oriented, because of the strong NOE observed for Me-26 and Me-25 (δ_H 0.896, s, 3H). HMBC cross-peak between Me-27 (δ_H 1.08, s, 3H) and C-16 (δ_C 27.2, t) and HSQC correlation for C-16 and H-16 allowed the assignment of H-16. The position of another sp^2 carbon (C-13) was determined by clear HMBC correlations of C-13 with H-19 (δ_H 1.30, m, 1H) and H-11 (δ_H 1.59, m, 1H). Unambiguous NOEs were observed for β-oriented Me-26

and H-12β (δ_H 1.86, m, 1H), H-12β and H-18 (δ_H 1.72, m, 1H), and H-18 and Me-27. Further detailed analyses of NMR data (Fig. S13.9) indicated structure of **52** as depicted in Figs. 4 and S13.9. This nortriterpene skeleton has not previously been isolated from nature. Compound **52** was previously prepared artificially from β-peltoboykinolic acid (β-amyrin homologue with a carboxyl group at the C-14 position) via heat treatment of the carboxylic acid at 230 °C, resulting in the production of **52** by CO_2 gas evolution.[14]

Detailed NMR analyses (600 MHz, C_6D_6) indicated that, like product **50**, **53** acetate had a β-amyrin skeleton, but with the C-14 Me group missing. The HMBC spectrum showed the following correlations: Me-26 (δ_H 0.974, s, 3H)/C-14 (δ_C 48.8, d), H-14 (δ_H 1.97, m, 1H)/C-13 (δ_C 141.1, s), H-14/C-12 (δ_C 121.1, d), H-18 (δ_H 2.16, dd, 12.9, 4.0 Hz)/C-13, H-18/C-12, and H-19 (δ_H 1.84, m, 1H)/C-13, verifying that the double-bond position was C-12/C-13. A clear NOE between H-9 (δ_H 1.00, m, 1H) and H-14 indicated that H-14 was α-oriented. Further detailed NMR analyses (Fig. S14.9) allowed us to propose that **53** was 27-nor-β-amyrin, as shown in Fig. 4 and S14.9.

A double bond was also involved in **54** acetate. Both Me-28 (δ_H 1.21, s, 3H) and Me-29 (δ_H 1.21, s, 3H) had HMBC cross-peaks for C-19 (δ_C 127.8, d), while Me-27 (δ_H 1.19, s, 3H) also exhibited HMBC correlation with C-18 (δ_C 144.6, s), supporting that the double-bond position was C-18/C-19. This finding suggested a germanicol skeleton for product **54**, as well as in the carbon framework of **51**. Unambiguous NOEs were found for Me-26 (δ_H 0.948, s, 3H)/H-13 (δ_H 2.07, br t, J=11.4 Hz, 1H)/Me-27 (δ_H 1.19, s, 3H), and for H-9 (δ_H 0.605, br d, J=11.4 Hz, 1H)/H-14 (δ_H 0.79, m, 1H), confirming the β-orientation of H-13 and α-disposition of H-14. These detailed analyses indicated that product **54** was 27-norgermanicol (see also Fig. S15.9).

We have previously reported the incubation experiment of **13** by EtAS and elucidated the structure of product **55**.[10,13] Isolation of product **56** was very difficult, because the conversion yield from **10** was significantly low (approx. 0.80%, see Fig. 3). Figure S16 shows the electron ionisation mass spectrometry (EIMS) results for product **56** (A) and authentic β-amyrin **2** (B). The mass spectrum of **56** was superimposable on that of **2**, except for the molecular weight (M^+), suggesting that product **56** had a β-amyrin scaffold. The fragment ions at *m*/*z* 203 and 218 present in the EIMS spectrum of **2**, were assigned as shown in Fig. S16 (C).[5d,15] These characteristic ions were also found in the spectrum of **56**, strongly indicating that substrate **10** underwent the full polycyclization reaction to yield **56**. Thus, product **56** can be proposed to be 26-nor-β-amyrin.

Discussion

All products, **49**–**54** and **56**, were produced from nor-oleanyl cations (**6'**, the final intermediates). Formation mechanisms are shown in Scheme 3. Products **50**, **53**, and **56**, possessing β-amyrin scaffolds, were generated as shown in Scheme 1, via 1,2-shifts of H-18 to the C-19 cation and H-13 to the C-18 cation in an antiperiplanar fashion, followed by H-12 proton elimination, affording the double bond at the C-12/C-13 position.

<Scheme 3>

Non-natural product **52** was produced by deprotonation at H-14, furnishing the double bond at C-13/C-14. Germanicol skeletons **51** and **54** were provided by deprotonation at H-18 in cation **6'**, affording the double bond at C-18/C-19. Notably, the major products of analogues **11** and **12** possess β-amyrin scaffolds, indicating that the less-bulky hydrogen atom substituents at C-10 and C-15 did not provide significant perturbation of the normal folding conformation of the substrates, although aberrant polycyclisation products, in which the double-bond positions were different, were also generated. The substantial amounts of products (22–34%, see Fig. 3) generated from **11** and **12** suggested that time-dependent inhibition by **11** and **12** was small or negligible. However, the conversion yield of analogue **10** was only 0.80%, clearly indicating that substrate analogue **10** underwent a time-dependent inhibition, as observed in the incubation experiment of **13**.[10] In contrast, analogues **7**–**9**, with the bulkier ethyl group (C_1-appendage) substituents at C-6, C-10, and C-15, underwent no cyclisation reaction, demonstrating that the EtAS enzyme was unable to accept the larger ethyl substituent. However, analogues **14**–**16**, with ethyl-group substituents at C-19 and C-23, did undergo polycyclisation, as we reported before.[10,12] The catalytic site domain responsible for the earlier cyclisation stages (mono-, bi-, and tricyclic stages) would be tightly packed (compact). Thus, the larger ethyl moieties could not be accepted due to steric repulsion, preventing cyclisation. This indicated that the correct size (Me group) at C-6, C-10, and C-15 positions in **1** is required for a normal polycyclisation cascade. Conversely, the catalytic domain involved in later cyclisation steps is somewhat loosely packed (less compact), and thus able to accommodate the bulkier ethyl group.

Next, we discuss the comparison of the substrate specificities of β-amyrin synthase (EtAS) and lanosterol synthases (LaS). Figures S17 and S18 depict the enzymatic products of analogues **7**–**18** by EtAS and LaS, respectively. The enzymatic cyclisation reactions of substrate analogues by β-amyrin synthase have only recently been disclosed.[7–12] In contrast, the many investigations into lanosterol synthase go

back to the 1960s. Corey *et al*. and van Tamelen *et al*. examined the cyclisation reactions of **1**[16] and **12** by LaS,[17] which were converted into 19-norlanosterol and 18-norlanosterol, respectively. Very recently, we reported the incubation experiment of **11** with LaS, resulting in the production of 30-norlanosterol and (14*E*,17*E*)-(13αH)-26-normalabarica-14,17,21-triene consisting of a 6/6/5-fused tricyclic ring system, with a product ratio of 9:1.[13] A normal folding conformation (*chair–boat–chair–chair*) and the correct backbone rearrangements resulted in production of the 30-norlanosterol scaffold. However, the minor tricyclic product was generated via an unusual *chair–chair–boat* folding conformation.[13] This suggested that replacement of the less bulky hydrogen atom at C-10 afforded the aberrant cyclisation product. Furthermore, bulky ethyl-substituted analogue **8** afforded some mono- and tricyclic products (see Fig. S18.1).[18] Thus, the correct steric bulk of Me-27 was required for the correct folding of **1** to yield lanosterol. Analogue **9** also underwent polycyclisation to afford the tricyclic product and homolanosterol with the Et group at C-13 (see Fig. S18.1), indicating that a precise steric bulk at C-15 was necessary for the normal folding conformation. LaS tolerated the bulky ethyl-substituted analogues (**8** and **9**), as described above, but EtAS never did accept the bulky analogues (**7**–**9**) as shown in Fig. 3, indicating that the reaction cavity of EtAS was more compact than that of LaS. Squalene is converted into hopene, which is produced by *Alicyclobacillus acidocaldarius* squalene-hopene cyclase (SHC).[2a, 2b] The hopane skeleton, consisting of the pentacyclic 6/6/6/6/5-fused ring system, is biosynthesised via the all-chair folding conformation of squalene. Figure S19 illustrates the enzymatic products of norsqualenes. 26-Norsqualene is transformed into 26-norhopene.[19] The incubation of 27-norsqualene by SHC affords unprecedented cyclisation products consisting of 6/5+5/5+(6) ring systems,[20] with a cyclisation pathway quite different to those of other triterpene cyclases. [20]28-Norsqualene afforded hopene and isohopene scaffolds as the enzymatic products, indicating that the effect of Me-28 on the cyclisation pathway was less significant than that of Me-27. The enzymatic reaction of 10(15)-ethyl-substituted squalene with SHC gave mono-, bi-, and tricyclic products, but did not afford tetra- or pentacyclic products (our unpublished results), indicating that the precise steric bulk at C-10 or C-15 was required for the normal squalene cyclisation pathway to occur. Detailed results will be reported in due course.

Conclusion

In summary, we have successfully investigated the influence of sterics on the polycyclisation pathway of oxidosqualene by β-amyrin synthase. Specifically, steric

bulk at the C-6, C-10, and C-15 positions was examined by substitution of the Me group with a less bulky hydrogen atom and a larger ethyl group. β-Amyrin synthase did not tolerate the bulkier ethyl-substituted analogues **7**–**9**, indicating that the catalytic domain responsible for the earlier cyclisation steps was tightly packed. Other triterpene cyclases, such as LaS and SHC, were able to accept **7**–**9** and their squalene analogues (deoxy-derivatives of **7**–**9**), respectively, to yield the cyclisation products. Thus, LaS and SHC had larger reaction spaces and more flexible substrate specificities than those of EtAS. The superiority of substrate flexibility by SHC is further supported by the fact that SHC can accept truncated analogues, such as farnesol and geranylgeraniol, as substrates,[22] but no or little reaction of the truncated analogues (epoxy-derivatives) occurred with EtAS (our unpublished results). However, abortive cyclisation products were accumulated by LaS and SHC without the polycyclisation going to completion. Therefore, the catalytic site domain involved in the earlier cyclisation steps was revealed to be significantly compact, irrespective of the type of triterpene cyclase. This tight binding of Me-26, Me-27, and Me-28 with the catalytic domains possibly leads to the highly efficient polycyclisation cascade of (oxido)squalene substrates.

Experimental

Analytical Methods

NMR spectra of the enzymatic products were recorded in C_6D_6 on a Bruker DMX 600 and DPX 400 spectrometers, the chemical shifts being given in ppm relative to the solvent peak δ_H =7.28 and δ_C=128.0 ppm as the internal reference for ^{1}H- and ^{13}C NMR spectra, respectively. The coupling constants *J* are given in Hz. GC analyses were done on a Shimadzu GC2014 chromatograph equipped with a flame ionization detector (a DB-1 capillary column, 30m x 0.25 mm x 0.25 μm, J&W Scientific. Inc.). GC-MS spectra were on a JEOL SX 100 or a JEOL JMS-Q1000 GC K9 instrument equipped with a ZB-5ms capillary column (30m x 0.25 mm x 0.25 μm; Zebron) by using the EI mode operated at 70 eV. High resolution-mass spectrometry (HR-MS) was performed on a JMS-T100GCV using electron ionization (EI) mode. HPLC was carried out with Hitachi L-1700 (pump) and L-7405 (UV detector), the HPLC peaks having been monitored at 210 or 214 nm. Specific rotation values were measured with a Horiba SEPA-300 polarimeter.

Incubation experiments of analogues 7~12.

The purification of EtAS and the incubation conditions were carried out according to

the published protocol. [4] The detailed incubation conditions are described in the text.

Synthetic experiments for substrate analogues 7~12

The detailed synthetic procedures and the spectral data of the synthetic compounds are described in Supporting Information.

Spectroscopic data of enzymatic products 49—54.

Product 49 acetate. ^{1}H NMR (600 MHz, C_6D_6): δ=0.810 (3H, s, Me-25), 0.874 (1H, dd, *J*=12.0, 2.0 Hz, H-5), 0.978 (3H, s, Me-28), 1.01 (1H, m, H-1), 1.05 (1H, m, H-11), 1.05 (6H, s, Me-23 & Me-24), 1.06 (1H, m, H-9), 1.12 (3H, s, Me-29), 1.17 (1H, m, H-7), 1.18 (1H, m, H-8), 1.20 (3H, s, Me-26), 1.23 (3H, s, Me-27), 1.30 (1H, m, H-6), 1.53 (1H, m, H-21), 1.54 (1H, m, H-16), 1.56 (1H, m, H-22), 1.57 (1H, m, H-15), 1.63 (1H, m, H-1), 1.66 (2H, m, H-16 & H-21), 1.67 (1H, m, H-22), 1.69 (1H, m, H-11), 1.70 (1H, m, H-2), 1.76 (1H, m, H-15), 1.83 (1H, m, ax.), 1.88 (3H, s, C*H*$_3$CO), 1.88 (2H, m, H-2 & H-6), 1.89 (1H, m, H-19), 1.91 (1H, m, H-7), 2.47 (1H, d, *J*=12.2 Hz, H-19), 2.78 (1H, bd, *J*=14.2 Hz, eq.), 4.85 (1H, dd, *J*=11.8, 4.2 Hz, H-3). ^{13}C NMR (150 MHz, C_6D_6): δ=14.3 (q, C-25), 17.1 (q, C-24), 20.7 (q, *C*H$_3$CO), 20.8 (q, C-26), 21.5 (t, C-6), 24.1 (q, C-28), 24.4 (t, C-2), 24.5 (q, C-27), 25.5 (t, C-12), 26.7 (t, C-11), 27.6 (t, C-7), 28.3 (q, C-23), 32.6 (q, C-29), 33.4 (s, C-20), 34.8 (t, C-15), 35.0 (s, C-17), 35.8 (t, C-21), 36.8 (s, C-10 & t, C-22), 37.4 (t, C-1), 37.9 (s, C-4), 38.9 (t, C-19), 39.1 (s, C-14), 39.7 (t, C-16), 48.7 (d, C-8), 50.1 (d, C-9), 54.3 (d, C-5), 80.6 (d, C-3), 131.6 (s, C-18), 137.7 (s, C-13), 169.9 (s, CH$_3$*C*O). MS (EI) of **49** (not acetate): see Fig. S10.1. HRMS (EI) of the acetate: *m*/*z*: calcd. for $C_{31}H_{50}O_2$: 454.38108; found: 454.38048; $[\alpha]_D^{20}$ = +22.4 (*c* = 0.12, $CHCl_3$)

Product 50 acetate. ^{1}H NMR (400 MHz, C_6D_6): δ=0.840 (3H, s, Me-25), 0.902 (1H, *J*=dd, 12.4, 2.8 Hz, H-5), 0.94 (1H, m, H-16), 0.98 (1H, m, H-1), 1.05 (3H, s, Me-23), 1.069 (6H, s, Me-24 & Me-27), 1.074 (3H, s, Me-29), 1.10 (3H, s, Me-28), 1.14 (1H, m, H-7), 1.17 (3H, s, Me-26), 1.26 (1H, m, H-9), 1.28 (1H, m, H-22), 1.34 (2H, m, H-6 & H-8), 1.36 (1H, m, H-19), 1.42 (1H, m, H-21), 1.49 (1H, m, H-1), 1.51 (1H, m, H-22), 1.56 (2H, m, H-15), 1.63 (1H, m, H-21), 1.64 (1H, m, H-6), 1.66 (1H, m, H-2), 1.83 (1H, m, H-7), 1.84 (1H, m, H-2), 1.88 (3H, s, C*H*$_3$CO), 1.93 (2H, m, H-11), 1.95 (1H, m, H-19), 2.18 (1H, m, H-16), 2.23 (1H, m, H-18), 4.83(1H, dd, *J*=11.6, 4.4 Hz, H-3), 5.47 (t, *J*=3.6 Hz, H-12). ^{13}C NMR (100 MHz, C_6D_6): δ=14.1 (q, C-25), 17.1 (q, C-24), 20.9 (q, *C*H$_3$CO), 21.1 (t, C-6), 22.8 (q, C-26), 23.8 (q, C-29), 24.2 (t, C-2), 24.9 (t, C-11), 26.1 (t, C-7), 27.4 (t, C-16), 28.3 (q, C-23), 28.8 (q, C-27), 31.3 (s, C-20), 32.9 (s, C-17), 33.6 (q, C-28), 34.7 (t, C-15), 35.0 (t, C-22), 35.9 (s, C-14), 36.9 (t, C-1), 37.1 (s, C-10),

37.2 (t, C-21), 37.8 (s, C-4), 44.8 (d, C-8), 45.9 (d, C-9), 46.2 (t, C-19), 48.7 (d, C-18), 54.3 (d, C-5), 80.6 (d, C-3), 123.1 (d, C-12), 146.2 (s, C-13), 169.9 (s, $CH_3\underline{C}O$). MS (EI) of **50** (not acetate): see Fig. S11.1. HRMS (EI) of the acetate: *m*/*z*: calcd. for $C_{31}H_{50}O_2$: 454.38108; found: 454.38107; $[\alpha]_D^{20}$ = +99.6 (*c* = 1.02, $CHCl_3$). m.p. 154─158°C.

Product 51 acetate. ^{1}H NMR (600 MHz, C_6D_6): δ=0.817 (3H, s, Me-26), 0.835 (1H, dd, *J*=12.4, 2.1 Hz, H-5), 0.882 (3H, s, Me-25), 0.92 (1H, m, H-9), 0.97 (1H, m, H-1), 1.03 (3H, s, Me-23), 1.04 (2H, m, H-7 & H-11), 1.07 (3H, s, Me-24), 1.17 (1H, m, H-8), 1.20 (6H, s, Me-28 & Me-29), 1.23 (3H, s, Me-27), 1.32 (1H, m, H-12), 1.33 (1H, m, H-6), 1.42 (1H, m, H-15), 1.51 (1H, m, H-16), 1.53 (1H, m, H-21), 1.58 (1H, m, H-16), 1.62 (1H, m, H-1), 1.63 (1H, m, H-22), 1.64 (1H, m, H-6), 1.65 (1H, m, H-12), 1.66 (1H, m, H-21), 1.68 (1H, m, H-23), 1.71 (1H, m, H-15), 1.72 (1H, m, H-11), 1.73 (1H, m, H-2), 1.88 (1H, m, H-2), 1.89 (3H, s, $C\underline{H_3}CO$), 1.93 (1H, m, H-7), 1.94 (1H, bd, *J*=11.8 Hz, H-13), 4.82 (1H, dd, *J*=11.8, 4.5 Hz, H-3), 5.19 (1H, s, H-19). ^{13}C NMR (150 MHz, C_6D_6): δ=13.1 (q, C-26), 14.3 (q, C-25), 17.1 (q, C-24), 20.9 (q, $\underline{C}H_3CO$), 21.6 (t, C-6), 24.4 (t, C-2), 24.8 (t, C-12), 25.4 (q, C-27), 25.5 (t, C-11), 27.2 (t, C-7), 28.3 (q, C-23), 29.4 (q, C-29), 31.5 (q, C-28), 32.6 (s, C-20), 33.8 (t, C-21), 34.6 (s, C-17), 35.6 (t, C-15), 36.8 (s, C-10), 37.2 (t, C-1), 37.3 (s, C-4), 37.9 (t, C-22), 38.1 (t, C-16), 39.4 (s, C-14), 46.3 (d, C-13), 47.2 (d, C-8), 49.3 (d, C-9), 54.4 (d, C-5), 80.6 (d, C-3), 129.9 (d, C-19), 142.4 (s, C-18), 169.9 (s, $CH_3\underline{C}O$). The assignment of C-28 and C-29 may be exchangeable, because of very similar chemical shifts. MS (EI) of **51** (not acetate): see Fig. S12.1. HRMS (EI) of the acetate: *m*/*z*: calcd. for $C_{31}H_{50}O_2$: 454.38020; found: 454.38107; $[\alpha]_D^{20}$ = +56.9 (*c* = 0.31, $CHCl_3$).

Product 52 acetate. ^{1}H NMR (600 MHz, C_6D_6): δ=0.77 (1H, dd, *J*=12.2, 2.0, H-5), 0.88(1H, m, H-1), 0.896 (3H, s, Me-25), 1.03 (1H, m, H-9), 1.035 (6H, s, Me-23 & Me-24), 1.05 (1H, m, H-16), 1.076 (3H, s, Me-27), 1.081(3H, s, Me-29), 1.09 (3H, s, Me-28), 1.10 (3H, s, Me-26), 1.18 (1H, ddd, *J*=12.6, 12.6, 3.6, H-7), 1.29 (1H, m, H-21), 1.30 (1H, m, H-19), 1.38 (1H, m, H-6), 1.42 (1H, m, H-22), 1.48 (1H, m, H-11), 1.54 (1H, m, H-6), 1.57 (1H, m, H-21), 1.59 (1H, m, H-11), 1.64 (1H, m, H-1), 1.67 (1H, m, H-22), 1.72 (1H, m, H-18), 1.73 (1H, m, H-19), 1.74 (1H, m, H-2), 1.86 (1H, m, H-12), 1.87 (1H, m, H-2), 1.88 (1H, m, H-7), 1.89 (3H, s, $C\underline{H_3}CO$), 2.09 (1H, m, H-15), 2.10 (1H, m, H-16), 2.19 (1H, m, H-15), 2.40 (1H, m, H-12), 4.80 (1H, dd, *J*=11.8, 4.5 Hz, H-3). ^{13}C NMR (150 MHz, C_6D_6): δ=16.6 (2C, q, C-24 & C-25), 18.1 (d, C-11), 18.7 (t, C-6), 20.3 (t, C-15), 20.6 (q, C-26), 20.8 (q, $\underline{C}H_3CO$), 24.1 (t, C-2), 24.7 (q, C-29), 27.2 (2C; q, C-27; t, C-16), 28.0 (q, C-23), 31.06 (s, C-20), 31.10 (s, C-17), 32.4 (t, C-12), 33.2 (q, C-28), 34.9 (t, C-21), 36.5 (t, C-22), 37.3 (s, C-4), 37.8 (t, C-1), 37.9 (s, C-10),

38.0 (s, C-8), 39.5 (t, C-7), 43.2 (t, C-19), 45.2 (d, C-18), 55.1 (d, C-5), 56.2 (d, C-9), 80.5 (d, C-3), 130.0 (s, C-13), 135.5 (s, C-14), 169.9 (s, $CH_3\underline{C}O$). The assignments of C-8 and C-10 and those of C-17 and C-20 may be exchangeable, because of the very close chemical shifts. MS (EI) of **52** (not acetate): see Fig. S13.1. HRMS (EI) of the acetate: *m*/*z*: calcd. for $C_{31}H_{50}O_2$: 454.38042; found: 454.38107; $[\alpha]_D^{20}$ = +168.6 (*c* = 0.06, $CHCl_3$).

Product 53 acetate. ^{1}H NMR (600 MHz, C_6D_6): δ=0.793 (1H, m, H-5), 0.862 (1H, ddd, *J*=13.0, 13.0, 3.6Hz, H-1), 0.934 (3H, s, Me-25), 0.974 (3H, s, Me-26), 1.00 (1H, m, H-9), 1.03 (1H, m, H-16), 1.04 (3H, s, Me-24), 1.06 (3H, s, Me-23), 1.086 (3H, s, Me-29), 1.09 (1H, m, H-7), 1.10 (3H, s, Me-27), 1.11 (3H, s, Me-28), 1.28 (1H, m, H-19), 1.29 (1H, m, H-21), 1.38 (2H, m, H-6 & H-22), 1.54 (1H, m, H-1), 1.55 (1H, m, H-6), 1.58 (2H, m, H-15 & H-21), 1.59 (1H, m, H-22), 1.70 (1H, m, H-2), 1.82 (1H, m, H-2), 1.84 (2H, m, H-11 & H-19), 1.88 (3H, s, $C\underline{H_3}CO$), 1.89 (1H, m, H-15), 1.93 (1H, m, H-7), 1.94 (1H, m, H-11), 1.97 (1H, m, H-14), 2.07 (1H, m, H-16), 2.19 (1H, dd, *J*=12.9, 4.0Hz, H-18), 4.81 (1H, dd, *J*=11.8, 4.5 Hz, H-3), 5.54 (1H, bs, H-12). ^{13}C NMR (150 MHz, C_6D_6): δ=15.3 (q, C-26), 16.3 (q, C-25), 16.9 (q, C-24), 18.7 (t, C-6), 20.7 (t, C-15), 20.83 (q, $\underline{C}H_3CO$), 22.82 (t, C-11), 24.0 (t, C-2), 24.5 (q, C-29), 28.2 (q, C-23), 28.4 (q, C-27), 29.4 (t, C-16), 31.2 (s, C-20), 32.8 (s, C-17), 33.5 (q, C-28), 34.8 (t, C-21), 35.7 (s, C-8), 36.89 (t, C-22), 36.94 (s, C-10), 37.9 (s, C-4), 38.1 (t, C-1), 41.8 (t, C-7), 44.7 (t, C-19), 48.2 (d, C-18), 48.8 (d, C-14), 55.39 (d, C-5), 55.43 (d, C-9), 80.4 (d, C-3), 121.1 (d, C-12), 141.1 (s, C-13), 169.9 (s, $CH_3\underline{C}O$). MS (EI) of **53** (not acetate): see Fig. S14.1. HRMS (EI) of the acetate: *m*/*z*: calcd. for $C_{31}H_{50}O_2$: 454.38057; found: 454.38107; $[\alpha]_D^{20}$ = +76.7 (*c* = 0.28, $CHCl_3$). m.p. 152─155°C.

Product 54 acetate. ^{1}H NMR (600 MHz, C_6D_6): δ=0.60 (1H, bd, *J*=11.4 Hz, H-9), 0.77 (1H, bd, *J*=11.3 Hz, H-5), 0.79 (1H, m, H-14)), 0.87 (1H, m, H-7), 0.88 (3H, s, Me-25), 0.90 (1H, m, H-1), 0.95 (3H, s, Me-26), 1.04 (3H, s, Me-24), 1.05 (3H, s, Me-23), 1.19 (3H, s, Me-27), 1.208 (3H, s, Me-29), 1.214 (3H, s, Me-28), 1.28 (1H, m, H-11), 1.35 (1H, m, H-6), 1.36 (1H, m, H-15), 1.40 (1H, m, H-16), 1.51 (1H, m, H-6), 1.54 (1H, m, H-21), 1.55 (2H, m, H-11 & H-12), 1.62 (1H, m, H-22), 1.63 (1H, m, H-1), 1.68 (2H, m, H-21 & H-22), 1.69 (1H, m, H-16), 1.75 (1H, m, H-2), 1.79 (1H, m, H-7), 1.889 (3H, s, $C\underline{H_3}CO$), 1.89 (1H, m, H-12), 1.92 (1H, m, H-2), 1.93 (1H, m, H-15), 2.07 (1H, bdd, *J*=11.4, 11.4 Hz, H-13), 4.84 (1H, dd, *J*=11.9, 4.5 Hz, H-3), 5.28 (1H, bs, H-19). The assignments of H-16 and H-22 may be exchangeable. ^{13}C NMR (150 MHz, C_6D_6): δ=15.1 (q, C-26), 16.7 (2C, q, C-24 & C-25), 18.5 (t, C-6), 20.76 (t, C-12), 20.79 (2C; q, $\underline{C}H_3CO$; t, C-11), 24.1 (t, C-2), 24.9 (q, C-27), 28.1 (q, C-23), 29.5 (q, C-29), 31.3 (t. C-15), 31.6 (q, C-28), 32.6 (s, C-20), 33.7 (t, C-21), 34.8 (s, C-17), 36.0 (d, C-13), 37.2

(s, C-10), 37.6 (s, C-8), 37.8 (t, C-22), 38.0 (s, C-4), 38.1 (t, C-1), 41.2 (t, C-7), 42.3 (t, C-16), 55.4 (d, C-5), 57.5 (d, C-14), 59.4 (d, C-9), 80.6 (d, C-3), 127.8 (d, C-19), 144.6 (s, C-18), 169.9 (s, $CH_3\underline{C}O$). The assignments of C-11 and C-12, those of C-16 and C-22 and those of C-28 and C-29 may be interchangeable, because of the very similar chemical shifts. MS (EI) of **54** (not acetate): see Fig. S15.1. HRMS (EI) of the acetate: *m*/z: calcd. for $C_{31}H_{50}O_2$: 454.38014; found: 454.38107; $[\alpha]_D^{20}$ = +43.8 (*c* = 0.05, $CHCl_3$).

Acknowledgements

This work was supported in part by Grant-in-Aid for Scientific Research from Japan Society for the Promotion of Science, Nos. 25450150 (C) and 18380001(B).

References

[1] A. Eschenmoser, L. Ruzicka, O. Jeger and D. Arigoni, *Helv. Chim. Acta* **1955**, *38*, 1890–1904.

[2] Review. (a) K. U. Wendt, G. E. Schulz, E. J. Corey and D. R Liu, *Angew. Chem., Int. Ed.* **2000**, *39*, 2812–2833. (b) T. Hoshino and T. Sato, *Chem. Commun.* **2002**, 291–301. (c) R. A. Yoder and J. N. Johnston, *Chem. Rev.* **2005**, *105*, 4730–4756. (d) I. Abe, *Nat. Prod. Rep.* **2007**, *24*, 1311–1331. (e) T.-K. Wu, C.-H. Chang, Y.-T. Liu and T.-T. Wang, *Chem. Rec.* **2008**, *8*, 302–325. (f) W. D. Nes, *Chem. Rev.* **2011**, *111*, 6423–6451.

[3] R. Xu, G. C. Fazio and S. P. T. Matsuda, *Phytochemistry* **2004**, *65*, 261–291.

[4] R. Ito, Y. Masukawa and T. Hoshino, *FEBS J.* **2013**, *280*, 1267–1280.

[5](a) Rees, H. H.; Mercer, E. I.; Goodwin, T. W., *Biochem. J.* **1966**, *99*, 726-734. (b) H. H. Rees, G. T. Britton and T. W. Goodwin, *Biochem. J.* **1968**, *106*, 659-665. (c) D. H. R. Barton, G. Mellows, D. A. Widdowson, and J. J. Wright, *J. Chem. Soc., C* **1971**, 1142-1148. (d) T. Suga and T. Shishibori, *Phytochemistry*, **1975**, *14*, 2411-2417. (e) S. Seo, Y. Tomita and K. Tori, *J. Am. Chem. Soc.*, **1981**, *103*, 2075-2780. (f) S. Seo, Y. Yoshimura, A. Uomori, K. Takeda, H. Seto, Y. Ebizuka and U. Sankawa, *J. Am. Chem. Soc.*, **1988**, *110*, 1740-1745.

[6] E. J. Corey and S. K. Gross, *J. Am. Chem. Soc.*, **1968**, *90*, 5045-5046.

[7] I. Abe, Sakano, H. Tanaka, W. Lou, H. Noguchi, M. Shibuya and Y. Ebizuka, *J. Am. Chem. Soc.*, **2004**, *126*, 3426-3427.

[8] I. Abe, Y. Sakano, M. Sodeyama, H. Tanaka, H. Noguchi, M. Shibuya and Y.

Ebizuka, *J. Am. Chem. Soc.*, **2004**, *126*, 6880–6881.
[9] H. Noma, H. Tanaka, H. Noguchi, M. Shibuya, Y. Ebizuka and I. Abe, *Tetrahedron Lett.*, **2004**, *45*, 8299-8301.
[10] T. Hoshino, Y. Yamaguchi, K. Takahashi, R. Ito, *Organic Lett.*, **2014**, *16*, 3548-3551.
[12] T. Hoshino, Y. Miyahara, M. Hanaoka, K. Takahashi, I. Kaneko, *Chem. Eur. J.* **2015**, *21*, 15769-15784.
[13] I. Kaneko and T. Hoshino, *J. Org. Chem.*, **2016**, *81*, 6657-6671.
[14] T. Hoshino, A. Chiba and N. Abe, *Chem. Eur. J.* **2012**, *18*, 13108-13116.
[15] M. Nagai, K. Izawa, T. Inoue, *Chem. Pharm. Bull*., **1969**, *17*, 1438-1443.
[16] (a) H. Budzikiewicz, J. M. Wilson and C. Djerassi, *J. Am. Chem. Soc.*, **1963**, *85*, 3688-3699. (b) J. Karlinen and C. Djerassi, *J. Org. Chem*., **1966**, *31*, 1945-1946.
[17] E. J. Corey, A. Krief, H. Yamamoto, *J. Am Chem. Soc*., **1971**, *93*, 1493-1494.
[18] E. E. van Tamlen, R. P. Hanzlik, K. B. Sharpless, R. B. Clayton, W. J. Richter, *J. Am Chem. Soc.*, **1968**, *90*, 3284-3286.
[19] T. Hoshino and Y. Sakai, *Tetrahedron Lett*., **2001**, *42*, 7319-7623.
[20] S. Nakano, S. Ohashi, and T. Hoshino, *Org. Biomol. Chem.*, **2004**, *2*, 2012-2022.
[21] T. Hoshino and S. Ohashi, *Org. Lett.*, **2002**, *4*, 2553-2556.
[22] T. Hoshino, Y. Kumai, I. Kudo, S. Nakano and S. Ohashi, *Org. Biomol. Chem.*, **2004**, *2*, 2650-2657.

Figures and Schemes

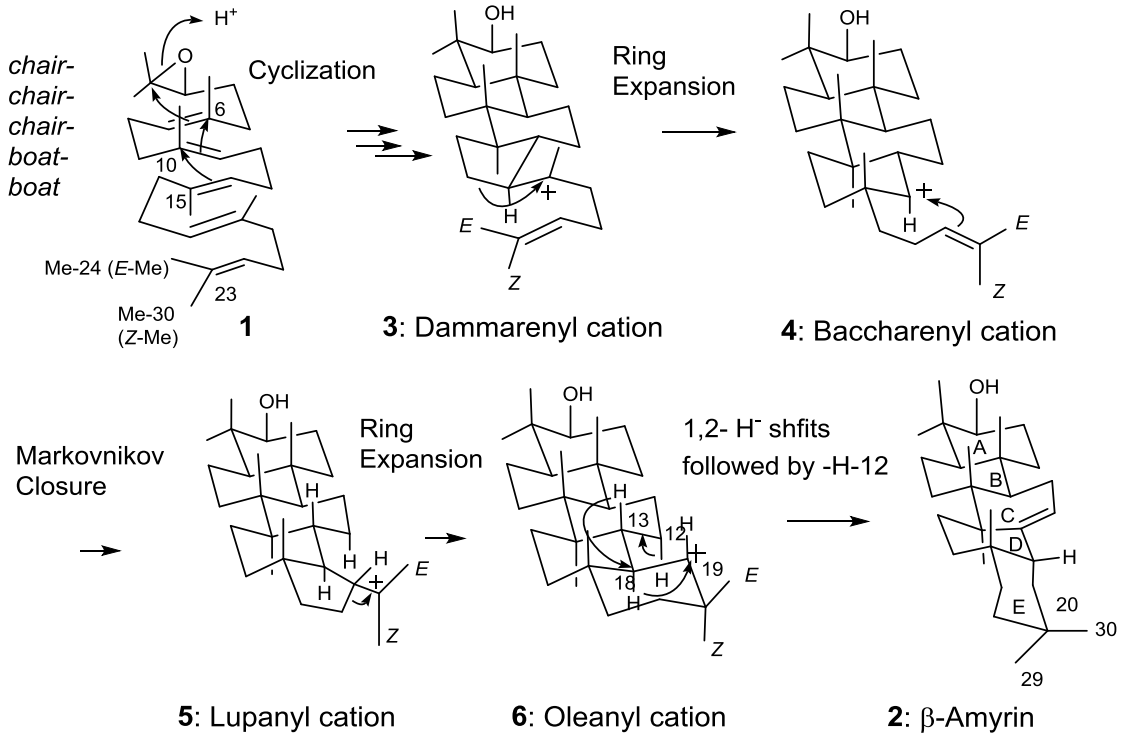

Scheme 1. Polycyclisation pathway of (3*S*)-2,3-oxidosqualene (**1**) into β-amyrin (**2**).

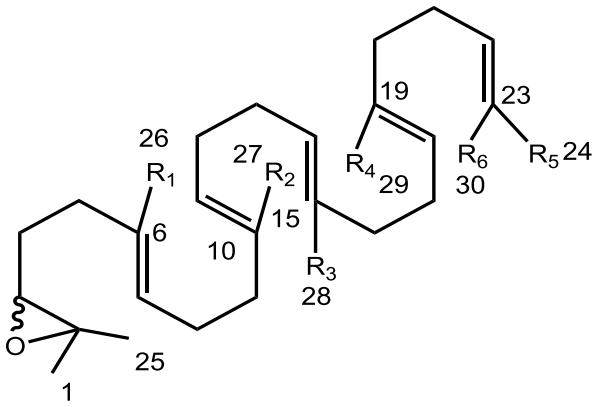

1: R_1=R_2=R_3=R_4=R_5=R_6=Me: 2,3-oxidosqualene
7: R_2=R_3=R_4=R_5=R_6=Me,R_1=Et: 6-ethyl-oxidosqualene (C_{31})
8: R_1=R_3=R_4=R_5=R_6=Me,R_2=Et: 10-ethyl-oxidosqualene (C_{31})
9: R_1=R_2=R_4=R_5=R_6=Me,R_3=Et: 15-ethyl-oxidosqualene (C_{31})
10: R_2=R_3=R_4=R_5=R_6=Me,R_1=H: 26-noroxidosqualene (C_{29})
11: R_1=R_3=R_4=R_5=R_6=Me,R_2=H: 27-noroxidosqualene (C_{29})
12: R_1=R_2=R_4=R_5=R_6=Me,R_3=H: 28-noroxidosqualene (C_{29})
13: R_1=R_2=R_3=R_5=R_6=Me,R_4=H: 29-noroxidosqualene (C_{29})
14: R_1=R_2=R_3=R_5=R_6=Me,R_4=Et: 19-ethyl-oxidosqualene (C_{31})
15:R_1=R_2=R_3=R_4=R_6=Me, R_5=Et: (23*E*)-ethyl-oxidosqualene (C_{31})
16:R_1=R_2=R_3=R_4=R_5=Me, R_6=Et: (23*Z*)-ethyl-oxidosqualene (C_{31})
17:R_1=R_2=R_3=R_4=R_6=Me, R_5=H: 24-noroxidosqualene (C_{29})
18:R_1=R_2=R_3=R_4=R_5=Me, R_6=H: 30-noroxidosqualene (C_{29})

Figure 1. Structures of substrate analogues discussed in the text.

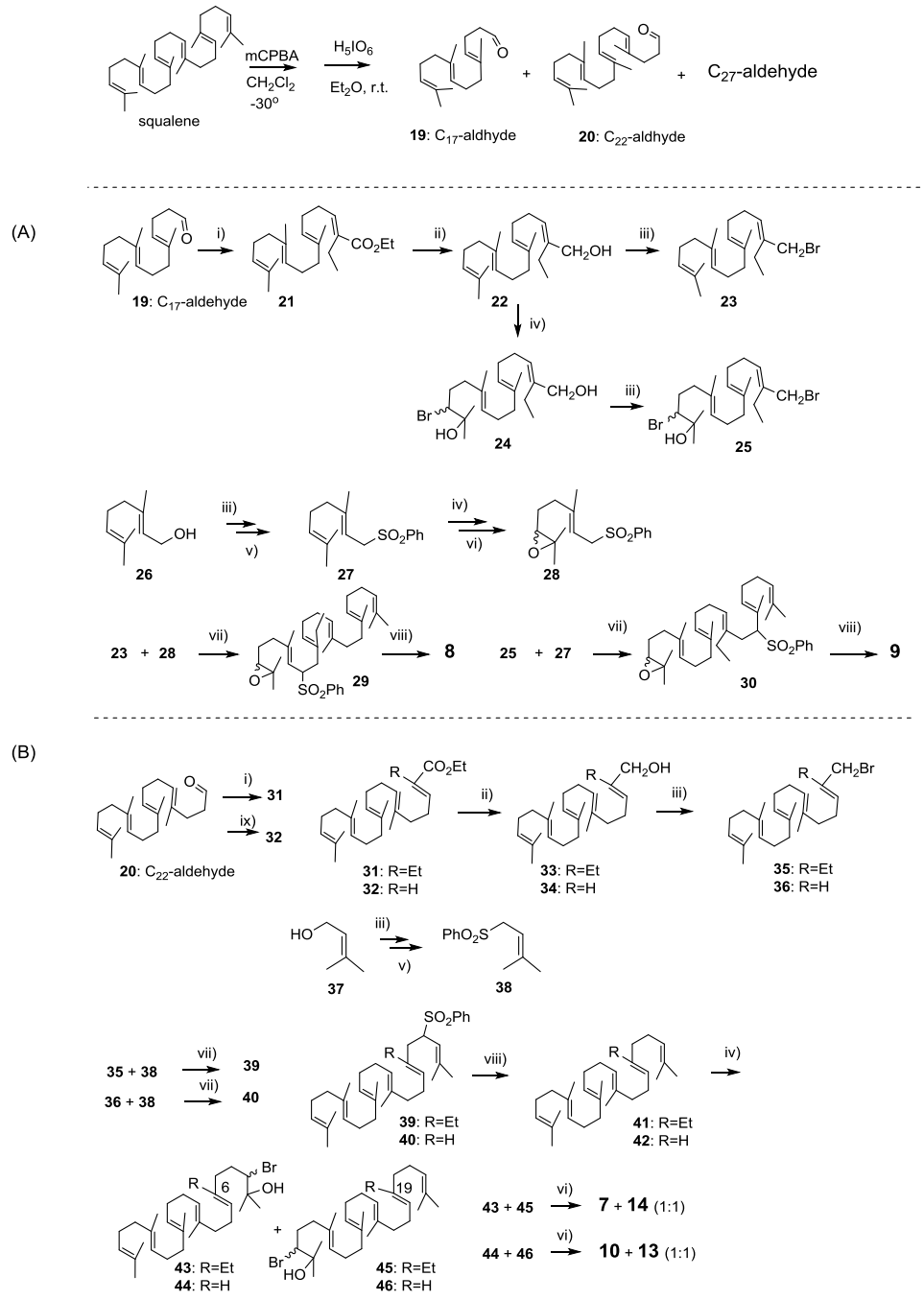

Scheme 2. Synthetic schemes for substrate analogues **8** and **9**, and mixtures of **7** and **14**, and **10** and **13**. (i) triethyl-2-phosphonobutyrate ($(EtO)_2P(O)CH(Et)CO_2Et$), *n*-BuLi, rt; (ii) $^{i}Bu_2AlH/Et_2O$, –40 °C; (iii) PBr_3, Et_2O, 0 °C; (iv) NBS, THF-H_2O, 0 °C; (v) $PhSO_2Na$, DMF, rt; (vi) K_2CO_3, MeOH, rt; (vii) *n*-BuLi, THF–HMPA (9:1), –78 °C; (viii) $LiBEt_3H$, Et_2O, $PdCl_3(dppp)$, 0 °C; (ix) triethyl-2-phosphonoacetate ($(EtO)_2P(O)CH_2CO_2Et$).

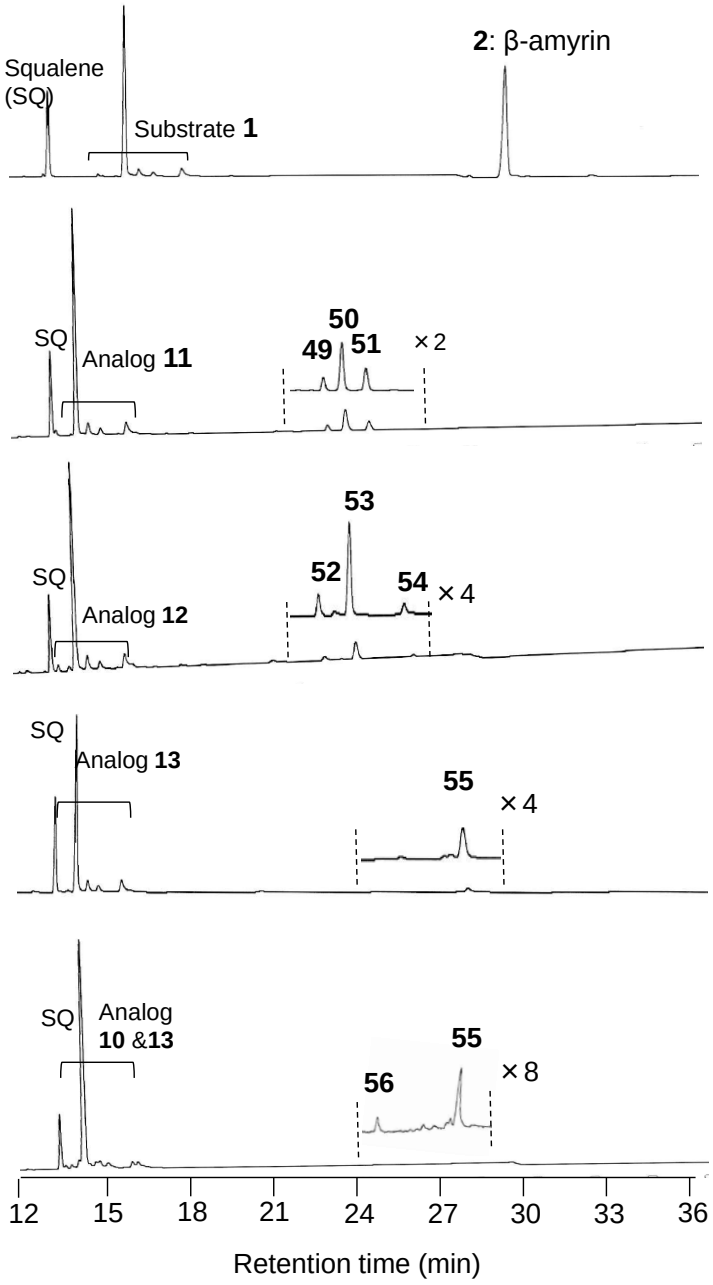

Figure 2. GC traces of hexane extracts from the incubation mixtures **1** and **11**–**13**, and a mixture of **10** and **13**. SQ denotes squalene (internal standard).
GC conditions: DB-1 capillary column (30 m × 0.25 mm); injection temp., 300 °C; column temp., 190–250 °C (10 °C/min) and 250–260°C (0.35 °C/min); flow rate (He gas), 1.50 mL/min.

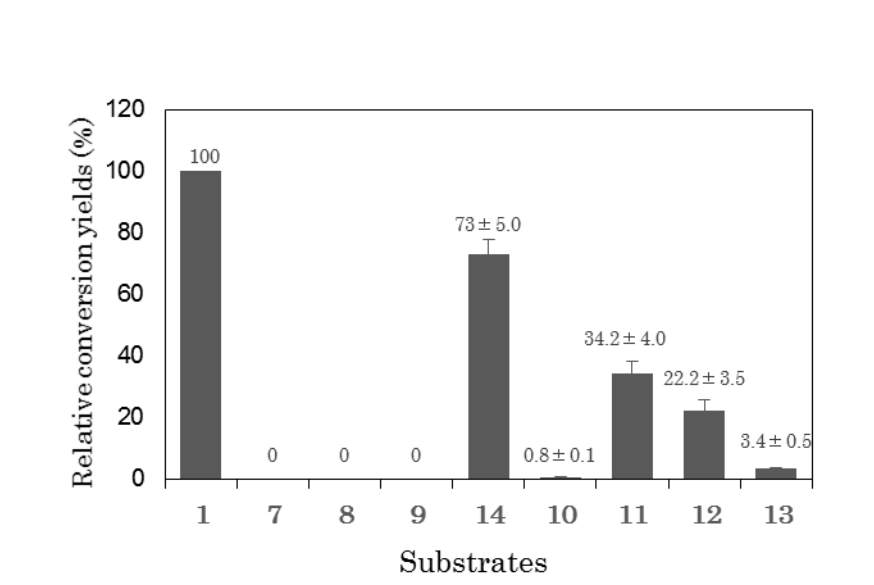

Figure 3. Conversion yields of substrate analogues relative to that of **1**. Relative activities were determined by estimating the total amounts of each product.

Substrate analogues **11** and **12** produced **49**–**51** and **52**–**54**, respectively. The production ratios were as follows: **49**/**50**/**51** = 1:4:2; **52**/**53**/**54** = 2:8:1. Conversion yields represent the total amounts of enzymatic products. Substrate **14** was converted into **47** and **48** in a 1:3 ratio, thus the total amount of **47** and **48** was calculated using the conversion yield of substrate **14**. A mixture of **10** and **13** (100 μg each) was incubated under the same conditions as the other substrates (5 μg EtAS at 30 °C for 9 h). Conversion yields for **10** and **13** were determined as 0.8% and 3.4%, respectively, from the peak areas of **56** and **55**.

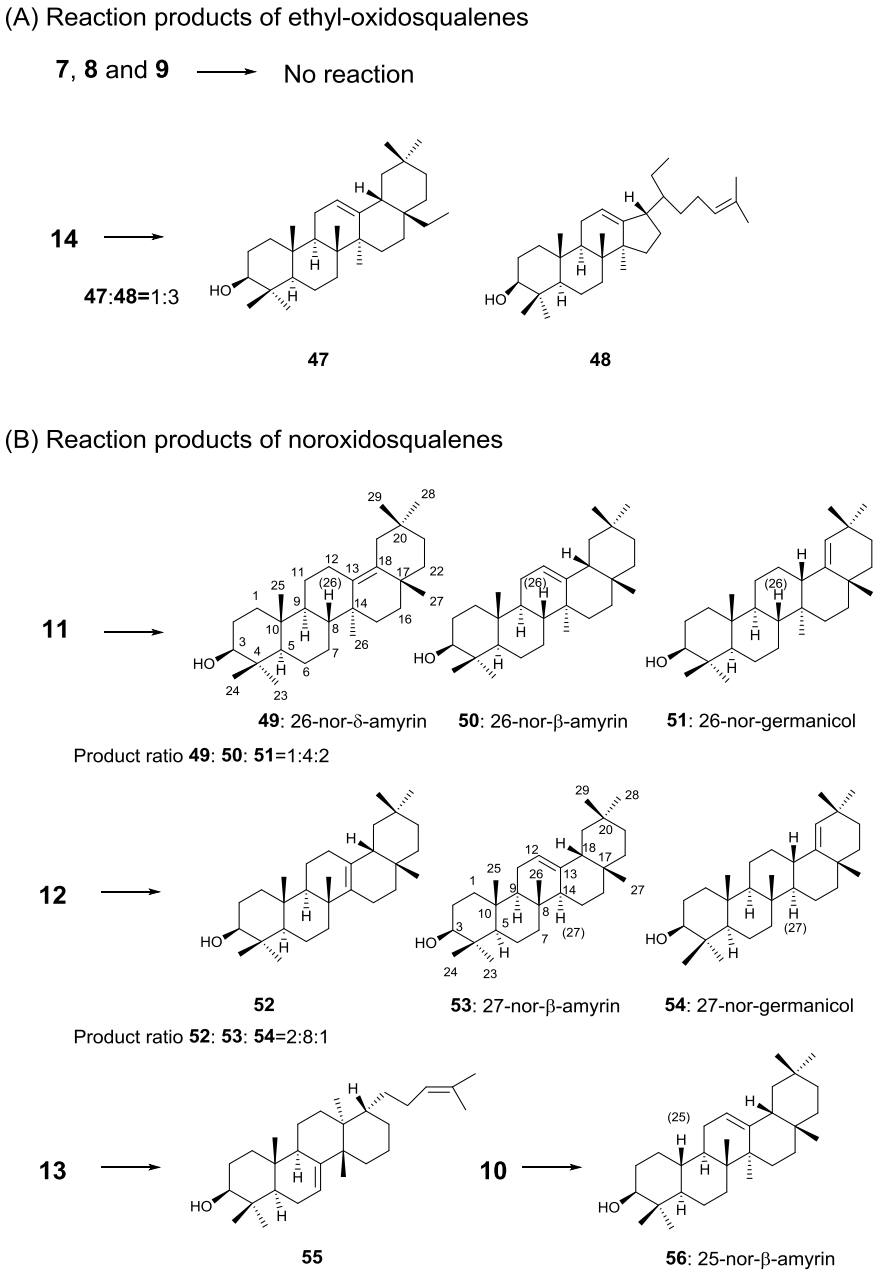

Figure 4. Products obtained from substrate analogues **7**–**14**. Carbon numbering systems are shown to aid interpretation of NMR data.

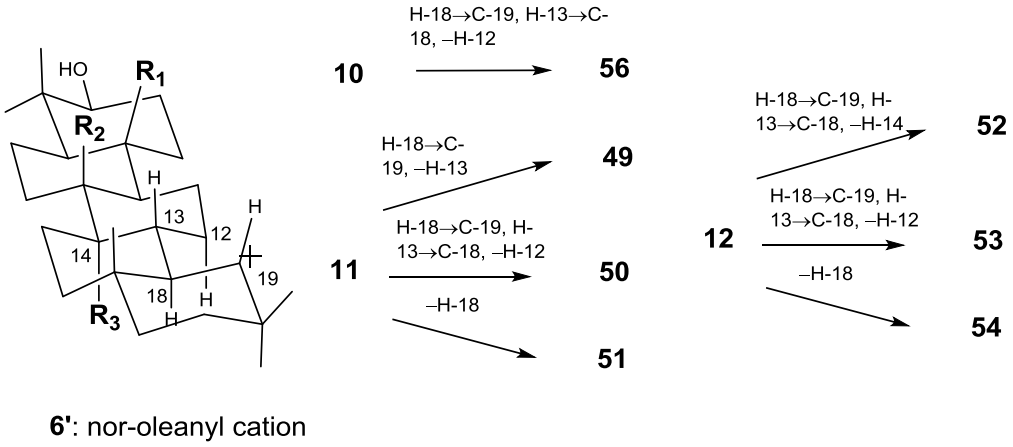

6': nor-oleanyl cation

Scheme 3. Enzymatic product formation mechanisms